Electro-optic detection of terahertz radiation

G. Gallot and D. Grischkowsky

School of Electrical and Computer Engineering and Center for Laser and Photonic Research, Oklahoma State University, Stillwater, Oklahoma 74078

Received January 8, 1999; revised manuscript received March 24, 1999

We present a complete frequency-domain description of electro-optic (EO) detection of terahertz (THz) electromagnetic radiation, including a description of the ellipsometry technique employed. These frequency-domain results show the effect of EO detection of a pulse of THz radiation as the product of three spectral filters acting on the complex amplitude spectrum of the THz pulse that is entering the EO crystal. For the usual experimental situation in which the optical bandwidth of the interrogating light pulse is small compared with the optical carrier frequency, we obtain an important simplification of our general result for the detected EO signal. When this simplified result is rewritten in the time domain, a more general description of the previous time-domain picture of EO detection is obtained. © 1999 Optical Society of America [S0740-3224(99)00308-2]

OCIS codes: 040.1880, 120.2130, 250.0250, 070.2580.

1. INTRODUCTION

The application of optoelectronic techniques to the generation and detection of terahertz (THz) electromagnetic radiation is now well established. These techniques have facilitated the widely practiced method of THz time-domain spectroscopy (THz TDS),[1] demonstrations of THz imaging,[2,3] and THz ranging.[4] THz TDS and THz ranging applications have usually used a photoconductive antenna for the THz receiver. THz imaging applications have used both photoconductive[2] and electro-optic detection.[3] Although electro-optic (EO) THz receivers have demonstrated exceptionally high-frequency performance,[5] they have not demonstrated the continuous spectral coverage of photoconductive receivers. This is so because of strong THz absorption and dispersion of the EO crystal, phase mismatch between the interrogating light pulse and the propagating THz pulse, and strong frequency dependence of the EO susceptibility. The comparison of photoconductive receivers with EO receivers is of significant interest, and experimental comparisons have been performed.[6,7]

Associated with these optoelectronic THz applications, it has become important to have a comprehensive understanding of the entire process of EO detection of THz radiation. Such understanding will permit a more meaningful comparison of the photoconductive and EO receivers and will elucidate the applicability of THz TDS with EO detection. Here we present a complete frequency-domain description of EO detection, including a description of the ellipsometry technique employed. These results, expressed as an easily evaluated Fourier integral, clearly show that the usual procedures of THz TDS are applicable independently of any time-domain distortion of the actual EO signal compared with the THz pulse.

For the usual experimental situation described by the slowly varying envelope approximation,[8] in which the optical bandwidth of the probing light pulse is small compared with the optical carrier frequency, we obtain an important simplification of our general result for the detected EO signal, expressed as a simple Fourier integral. When this simplified integral is rewritten in the time domain, we obtain a more general description of the intuitive time-domain picture that was introduced by Bakker *et al.*[9] Restricting our result to the frequency-independent EO susceptibility situation considered by Bakker *et al.*,[9] we identically obtain their intuitive picture, in which the EO signal is given by a cross correlation between the interrogating optical pulse traveling at the optical group velocity and the propagating THz pulse integrated over the EO crystal length.

2. SUM- AND DIFFERENCE-FREQUENCY MIXING

As we show below, EO detection of THz radiation is based on the measurement of the phase modulation induced on the interrogating light pulse by the THz pulse as both pulses mutually propagate through the EO crystal. This phase modulation is more precisely understood as the generation of phase-coherent sidebands on the spectrum of the optical pulse, through the generation of sum- and difference-frequency components.

We now discuss the generation of these sum- and difference-frequency components in the EO crystal as a result of the interaction between the propagating light pulse and the propagating THz pulse. The notation and theoretical presentation follows that of Shen[8] as closely as possible.

The fields that we consider are defined as follows:

Terahertz field

$$\mathbf{E}_1(z', \omega_1) = E_1(z', \omega_1)\hat{u}_j, \tag{1}$$

$$E_1(z', \omega_1) = A_1(z', \omega_1) \times \exp[ik_1(\omega_1)z'] \times \exp(-i\omega_1 t),$$

$$E_1(z', t) = \int_{-\infty}^{+\infty} E_1(z', \omega_1)\mathrm{d}\omega_1. \tag{2}$$

0740-3224/99/081204-09$15.00

Optical beam
$$\mathbf{E}_2(z', \omega_2) = E_2(z', \omega_2)\hat{u}_k, \quad (3)$$
$$E_2(z', \omega_2) = A_2(z', \omega_2 - \omega_0)\exp[ik_2(\omega_2)z']\exp[-i(\omega_2 - \omega_0)t],$$
$$E_2(z', t) = \int_{-\infty}^{+\infty} E_2(z', \omega_2 - \omega_0)\mathrm{d}\omega_2. \quad (4)$$

Sum-frequency field
$$\mathbf{E}_3(z', \omega_3) = E_3(z', \omega_3)\hat{u}_i, \quad (5)$$
$$E_3(z', \omega_3) = A_3(z', \omega_3 - \omega_0)\exp[ik_3(\omega_3)z']\exp[-i(\omega_3 - \omega_0)t],$$
$$E_3(z', t) = \int_{-\infty}^{+\infty} E_3(z', \omega_3 - \omega_0)\mathrm{d}\omega_3. \quad (6)$$

Difference-frequency field
$$\mathbf{E}_4(z', \omega_4) = E_4(z', \omega_4)\hat{u}_i, \quad (7)$$
$$E_4(z', \omega_4) = A_4(z', \omega_4 - \omega_0)\exp[ik_4(\omega_4)z']\exp[-i(\omega_4 - \omega_0)t],$$
$$E_4(z', t) = \int_{-\infty}^{+\infty} E_4(z', \omega_4 - \omega_0)\mathrm{d}\omega_4. \quad (8)$$

The specific notation used is the following:

Sum frequency $\omega_3 = \omega_2 + \omega_1$,

Difference frequency $\omega_4 = \omega_2 - \omega_1$.

Subscripts i, j, and k refer to the generalized crystallographic axes of the crystal x', y', and z', respectively. ω_0 is the optical carrier frequency. With absorption, the wave vectors become complex; then

$$k = k' + i\beta, \quad (9)$$

where β is the attenuation coefficient.

Electro-Optic Polarization The polarization generated at sum frequency ω_3 at position z by the field amplitudes $E_1(\omega_1)$ and $E_2(\omega_2)$ as a result of the nonlinear susceptibility of the EO crystal is given by

$$\mathbf{P}_+^{(2)}(\omega_3) = p_+^{(2)}\exp[i(k_1 + k_2)z' - i\omega_3 t]\hat{u}_+ = \chi_{ijk}^{(2)}(\omega_3)E_1(\omega_1)E_2(\omega_2)\hat{u}_+, \quad (10)$$

where $p_+^{(2)}$ designates the polarization amplitude. Similarly, we obtain for the difference frequency

$$\mathbf{P}_-^{(2)}(\omega_4) = p_-^{(2)}\exp[i(-k_1 + k_2)z' - i\omega_4 t]\hat{u}_- = \chi_{ijk}^{(2)}(\omega_4)E_1^*(\omega_1)E_2(\omega_2)\hat{u}_-, \quad (11)$$

where $\hat{u}_+$ and $\hat{u}_-$ are generalized unit vectors that represent any one of $\hat{u}_{x'}$, $\hat{u}_{y'}$, or $\hat{u}_{z'}$.

Using the slowly varying amplitude approximation for the pulsed optical fields A_3 and A_4, we write these generated fields with the sum and the difference frequencies, respectively, as[8]

$$\left[\frac{\partial}{\partial z'} + \beta_3(\omega_3)\right]A_3(z', \omega_3 - \omega_0) = i\frac{2\pi\omega_3^2}{c^2k_3'(\omega_3)}p_+^{(2)}\exp\{i\Delta k_+'z' - [\beta_1(\omega_1) + \beta_2(\omega_2)]z'\}, \quad (12)$$

$$\left[\frac{\partial}{\partial z'} + \beta_4(\omega_4)\right]A_4(z', \omega_4 - \omega_0) = i\frac{2\pi\omega_4^2}{c^2k_4'(\omega_4)}p_-^{(2)}\exp\{i\Delta k_-'z' - [\beta_1(\omega_1) + \beta_2(\omega_2)]z'\}, \quad (13)$$

where the phase-matching conditions are determined by the real part of k:

$$\Delta k_+' = -k_3'(\omega_2 + \omega_1) + k_1'(\omega_1) + k_2'(\omega_2), \quad (14)$$

$$\Delta k_-' = -k_4'(\omega_2 - \omega_1) - k_1'(\omega_1) + k_2'(\omega_2). \quad (15)$$

Solution of Eq. (12) for an EO crystal of length l yields

$$A_3(l, \omega_3 - \omega_0) = i\frac{2\pi\omega_3^2}{c^2k_3'(\omega_3)}p_+^{(2)}\frac{\exp\{i\Delta k_+'l - [\beta_1(\omega_1) + \beta_2(\omega_2)]l\} - \exp[-\beta_3(\omega_3)l]}{i\Delta k_+' - [\beta_1(\omega_1) + \beta_2(\omega_2) - \beta_3(\omega_3)]}. \quad (16)$$

By using Eq. (10) and the complete k vector including absorption, we can rewrite Eq. (16) as

$$A_3(l, \omega_3 - \omega_0) = i\frac{2\pi\omega_3^2}{c^2k_3'(\omega_3)}\chi_{ijk}^{(2)}(\omega_3)\frac{[\exp(i\Delta k_+l) - 1]}{i\Delta k_+} \times \exp[-\beta_3(\omega_3)l]A_1(\omega_1)A_2(\omega_2 - \omega_0). \quad (17)$$

Similarly for Eq. (13),

$$A_4(l, \omega_4 - \omega_0) = i\frac{2\pi\omega_4^2}{c^2 k_4'(\omega_4)} p_-^{(2)} \frac{\exp\{i\Delta k_- l - [\beta_1(\omega_1) + \beta_2(\omega_2)]l\} - \exp[-\beta_4(\omega_4)l]}{i\Delta k_- - [\beta_1(\omega_1) + \beta_2(\omega_2) - \beta_4(\omega_4)]}, \quad (18)$$

which is equivalent to

$$A_4(l, \omega_4 - \omega_0) = i\frac{2\pi\omega_4^2}{c^2 k_4'(\omega_4)} \chi_{ijk}^{(2)}(\omega_4) \frac{\exp(i\Delta k_- l) - 1}{i\Delta k_-} \times \exp[-\beta_4(\omega_4)l] A_1^*(\omega_1) A_2(\omega_2 - \omega_0), \quad (19)$$

where the complex phase mismatch and absorption are

$$\Delta k_+ = -k_3(\omega_2 + \omega_1) + k_1(\omega_1) + k_2(\omega_2), \quad (20)$$

$$\Delta k_- = -k_4(\omega_2 - \omega_1) - k_1(\omega_1) + k_2(\omega_2) \quad (21)$$

and at the inside face of the EO crystal

$$A_n(\omega) = A_n(z' = 0, \omega). \quad (22)$$

As will be shown in the following discussion, there are three optical fields with the same frequency ω: $E_2(\omega)$ from the undepleted optical beam, $E_3(\omega)$ resulting from sum-frequency generation, and $E_4(\omega)$ resulting from difference-frequency generation. For $E_3(\omega)$ and $E_4(\omega)$, the fields radiated at frequency ω are obtained from the results of Eqs. (17) and (19), with

$\omega_1 = \Omega$ and $\omega_2 = \omega - \Omega$ (sum frequency),

$\omega_1 = \Omega$ and $\omega_2 = \omega + \Omega$ (difference frequency),

$k_3(\omega) = k_4(\omega)$.

The total fields E_3 and E_4 radiated at ω by sum- and difference-frequency generation, respectively, are then obtained by integration over the THz range determined by the bandwidth of the THz pulse:

$$E_3(l, \omega) = i\int_{-\infty}^{+\infty} \frac{2\pi\omega^2}{c^2 k_3'(\omega)} \chi_{ijk}^{(2)}(\omega; \Omega, \omega - \Omega) \times \left[\frac{\exp(i\Delta k_+ l) - 1}{i\Delta k_+}\right] \exp[ik_3(\omega)l] A_1(\Omega) \times \exp[-i\Omega(t + \tau)] A_2(\omega - \Omega - \omega_0) \times \exp[-i(\omega - \Omega - \omega_0)t] d\Omega, \quad (23)$$

$$E_4(l, \omega) = i\int_{-\infty}^{+\infty} \frac{2\pi\omega^2}{c^2 k_3'(\omega)} \chi_{ijk}^{(2)}(\omega; \Omega, \omega + \Omega) \times \left[\frac{\exp(i\Delta k_- l) - 1}{i\Delta k_-}\right] \exp[ik_3(\omega)l] A_1^*(\Omega) \times \exp[+i\Omega(t + \tau)] A_2(\omega + \Omega - \omega_0) \times \exp[-i(\omega + \Omega - \omega_0)t] d\Omega, \quad (24)$$

where, as illustrated in Fig. 3 below, τ is the relative delay between the optical and the THz pulses. Then

$$E_3(l, \omega) = i\left\{\int_{-\infty}^{+\infty} \frac{2\pi\omega^2}{c^2 k_3'(\omega)} \chi_{ijk}^{(2)}(\omega; \Omega, \omega - \Omega) \times \left[\frac{\exp(i\Delta k_+ l) - 1}{i\Delta k_+}\right] \times A_1(\Omega) A_2(\omega - \Omega - \omega_0) \exp(-i\Omega\tau) d\Omega\right\} \times \exp[ik_3(\omega)l - i(\omega - \omega_0)t], \quad (25)$$

$$E_4(l, \omega) = i\left\{\int_{-\infty}^{+\infty} \frac{2\pi\omega^2}{c^2 k_3'(\omega)} \chi_{ijk}^{(2)}(\omega; \Omega, \omega + \Omega) \times \left[\frac{\exp(i\Delta k_- l) - 1}{i\Delta k_-}\right] \times A_1^*(\Omega) A_2(\omega + \Omega - \omega_0) \exp(+i\Omega\tau) d\Omega\right\} \times \exp[ik_3(\omega)l - i(\omega - \omega_0)t]. \quad (26)$$

The total field radiated at frequency ω is then, by superposition,

$$E_3 + E_4 = i\int_{-\infty}^{+\infty} \frac{2\pi\omega^2}{c^2 k_3'(\omega)} \exp[ik_3(\omega)l] \left\{\chi_{ijk}^{(2)}(\omega; \Omega, \omega - \Omega) \times \left\{\frac{\exp[i\Delta k_+(\Omega, \omega)l] - 1}{i\Delta k_+(\Omega, \omega)}\right\} A_1(\Omega) A_2(\omega - \Omega - \omega_0) \times \exp(-i\Omega\tau) + \chi_{ijk}^{(2)}(\omega; \Omega, \omega + \Omega) \times \left\{\frac{\exp[i\Delta k_-(\Omega, \omega)l] - 1}{i\Delta k_-(\Omega, \omega)}\right\} \times A_1^*(\Omega) A_2(\omega + \Omega - \omega_0) \exp(i\Omega\tau)\right\} \times \exp[-i(\omega - \omega_0)t] d\Omega. \quad (27)$$

Replacing Ω by $-\Omega$ within the second set of braces in Eq. (27) and using the relations

$$\Delta k_-(-\Omega, \omega) = \Delta k_+(\Omega, \omega), \quad (28)$$

$$A_1^*(-\Omega) = A_1(\Omega), \quad (29)$$

$$\chi_{ijk}^{(2)}(\omega; -\Omega, \omega + \Omega) = \chi_{ijk}^{(2)*}(\omega; \Omega, \omega + \Omega), \quad (30)$$

we obtain

$$E_3 + E_4 = i\int_{-\infty}^{+\infty} \frac{2\pi\omega^2}{c^2 k_3'(\omega)} \exp[ik_3(\omega)l] \times [\mathrm{Re}\,\chi_{ijk}^{(2)}(\omega; \Omega, \omega - \Omega)] \times \left\{\frac{\exp[i\Delta k_+(\Omega, \omega)l] - 1}{i\Delta k_+(\Omega, \omega)}\right\} \times A_1(\Omega)A_2(\omega - \Omega - \omega_0) \times \exp[-i\Omega\tau - i(\omega - \omega_0)t]\mathrm{d}\Omega. \quad (31)$$

Assuming that there is no depletion of energy from the pump waves, the total optical field $\mathbf{E}(\omega)$ is the sum of the three components

$$\mathbf{E}(\omega) = \mathbf{E}_2(\omega) + \mathbf{E}_3(\omega) + \mathbf{E}_4(\omega). \quad (32)$$

After projection depending on the geometry and spatial orientation of a particular crystal, we introduce the new axes $\hat{\mathbf{e}}_x$, $\hat{\mathbf{e}}_y$, and $\hat{\mathbf{e}}_z$. Then the effective nonlinearities χ_{eff}^x and χ_{eff}^y describe the nonlinear propagation in directions $\hat{\mathbf{e}}_x$ and $\hat{\mathbf{e}}_y$. For the crystals usually employed, χ_{eff} is proportional to only one χ_{ijk}, depending on the symmetry of the crystal. $E_{3x} + E_{4x}$ and $E_{3y} + E_{4y}$ are the fields radiated in the directions of polarization $\hat{\mathbf{e}}_x$ and $\hat{\mathbf{e}}_y$, respectively. Then let E_x and E_y be the components of $\mathbf{E}$ relative to $\hat{\mathbf{e}}_x$ and $\hat{\mathbf{e}}_y$. At the output of the crystal,

$$\mathbf{E}_2(\omega) = E_{2x}\hat{\mathbf{e}}_x + E_{2y}\hat{\mathbf{e}}_y = A_{2x}\exp[ik_x(\omega)l - i(\omega - \omega_0)t]\hat{\mathbf{e}}_x + A_{2y}\exp[ik_y(\omega)l - i(\omega - \omega_0)t]\hat{\mathbf{e}}_y, \quad (33)$$

$$E_x(\omega) = E_{2x}(\omega) + E_{3x}(\omega) + E_{4x}(\omega), \quad (34)$$

$$E_y(\omega) = E_{2y}(\omega) + E_{3y}(\omega) + E_{4y}(\omega), \quad (35)$$

with

$$E_{3x} + E_{4x} = i\int_{-\infty}^{+\infty} \frac{2\pi\omega^2}{c^2 k'(\omega)} \exp[ik_x(\omega)l]\chi_{\mathrm{eff}}^x(\omega; \Omega, \omega - \Omega) \times \left\{\frac{\exp[i\Delta k_+(\Omega, \omega)l] - 1}{i\Delta k_+(\Omega, \omega)}\right\} \times A_1(\Omega)A_2(\omega - \Omega - \omega_0) \times \exp[-i\Omega\tau - i(\omega - \omega_0)t]\mathrm{d}\Omega, \quad (36)$$

$$E_{3y} + E_{4y} = i\int_{-\infty}^{+\infty} \frac{2\pi\omega^2}{c^2 k'(\omega)} \exp[ik_y(\omega)l]\chi_{\mathrm{eff}}^y(\omega; \Omega, \omega - \Omega) \times \left\{\frac{\exp[i\Delta k_+(\Omega, \omega)l] - 1}{i\Delta k_+(\Omega, \omega)}\right\} A_1(\Omega)A_2(\omega - \Omega - \omega_0) \times \exp[-i\Omega\tau - i(\omega - \omega_0)t]\mathrm{d}\Omega. \quad (37)$$

We now connect the coherent sum and difference mixing with phase modulation of the propagating optical pulse by the definitions

$$E_x(\omega) \equiv E_{2x}(\omega)[1 + i\varphi_x(\omega, \tau)], \quad (38)$$

$$E_y(\omega) \equiv E_{2y}(\omega)[1 + i\varphi_y(\omega, \tau)], \quad (39)$$

where the phase modulation is given by

$$\varphi_x(\omega, \tau) = \frac{E_{3x}(l, \omega) + E_{4x}(l, \omega)}{iE_{2x}(\omega)}, \quad (40)$$

$$\varphi_y(\omega, \tau) = \frac{E_{3y}(l, \omega) + E_{4y}(l, \omega)}{iE_{2y}(\omega)}. \quad (41)$$

When we assume that the total dephasings φ_x and φ_y are small compared with 1, Eqs. (38) and (39) yield

$$E_x(\omega) = E_{2x}(\omega)\exp[i\varphi_x(\omega, \tau)], \quad (42)$$

$$E_y(\omega) = E_{2y}(\omega)\exp[i\varphi_y(\omega, \tau)]. \quad (43)$$

These results are now in a form to enable us to understand the physical basis of EO detection as phase modulation of the optical pulse caused by the electric field of the THz pulse by means of the coupling of the EO crystal. In Section 3 we present the technique of ellipsometry used for the measurement of this phase modulation.

3. MEASUREMENT OF PHASE MODULATION BY ELLIPSOMETRY

Let us now consider the measurement of phase modulation by ellipsometry, as illustrated in Fig. 1. For a monochromatic wave, the general solution can be found in Ref. 10, where the incoming field components referenced to the axes of the $\lambda/4$ plate are

$$E_x = a_0(\omega)\cos[k(\omega)z - \omega t + \varphi_x(\omega)],$$

$$E_y = a_0(\omega)\cos[k(\omega)z - \omega t + \varphi_y(\omega)], \quad (44)$$

where φ_x and φ_y are the dephasing for both components of the electric field.

For our specific example the $\lambda/4$ plate adds a $\pi/2$ dephasing on axis Y. Subsequent analysis by a suitably oriented Wollaston polarizer gives the intensities of the two components of the resultant elliptically polarized light (see Figs. 1 and 2). The difference of the two intensities gives the measured signal.

The field components after the $\lambda/4$ plate are

$$E_x = a_0(\omega)\cos[k(\omega)z - \omega t + \varphi_x(\omega)],$$

$$E_y = a_0(\omega)\cos[k(\omega)z - \omega t + \varphi_y(\omega) + (\pi/2)]. \quad (45)$$

Defining the dephasing φ equal to $\varphi_y - \varphi_x$ and assuming that φ is small, we obtain the major and minor axes of the polarization ellipse after the plate (see Fig. 2):

$$a(\omega) = a_0(\omega)[1 + {}^1/_2\varphi(\omega)],$$

$$b(\omega) = a_0(\omega)[1 - {}^1/_2\varphi(\omega)]. \quad (46)$$

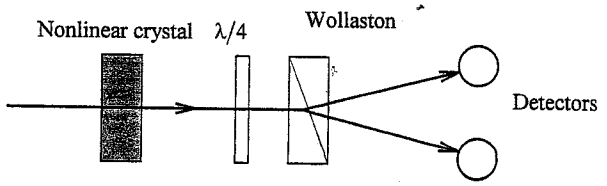

Fig. 1. Ellipsometer with a $\lambda/4$ plate and a Wollaston polarizer.

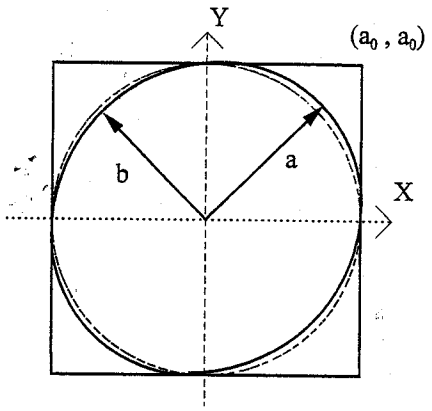

Fig. 2. Polarization ellipse (solid curve) for the electric field after the λ/4 plate, compared with a circle (dashed curve).

After the Wollaston polarizer, both intensities I_a and I_b are detected:

$$I_a = {}^1/_2\epsilon_0 c \int_0^{+\infty} |a(\omega)|^2 \mathrm{d}\omega,$$

$$I_b = {}^1/_2\epsilon_0 c \int_0^{+\infty} |b(\omega)|^2 \mathrm{d}\omega. \tag{47}$$

Hence

$$\frac{2}{\epsilon_0 c} I_a = \int_0^{+\infty} |a_0(\omega)|^2 \mathrm{d}\omega + {}^1/_4 \int_0^{+\infty} |a_0(\omega)\varphi(\omega)|^2 \mathrm{d}\omega + \mathrm{Re} \int_0^{+\infty} |a_0(\omega)|^2 \varphi(\omega) \mathrm{d}\omega, \tag{48}$$

$$\frac{2}{\epsilon_0 c} I_b = \int_0^{+\infty} |a_0(\omega)|^2 \mathrm{d}\omega + {}^1/_4 \int_0^{+\infty} |a_0(\omega)\varphi(\omega)|^2 \mathrm{d}\omega - \mathrm{Re} \int_0^{+\infty} |a_0(\omega)|^2 \varphi(\omega) \mathrm{d}\omega. \tag{49}$$

Then the signal S is equal to

$$S = I_a - I_b = \epsilon_0 c \, \mathrm{Re} \int_0^{+\infty} |a_0(\omega)|^2 \varphi(\omega) \mathrm{d}\omega. \tag{50}$$

4. DETECTION OF THE ELECTRO-OPTIC SIGNAL BY ELLIPSOMETRY

We can now adapt the results of Section 2 to the situation considered in Section 3 to calculate the measured EO signal. For this we consider the case when the generated electric fields come from a nonlinear process in an isotropic nonlinear crystal. For this crystal the linear and the nonlinear properties are assumed to be independent of polarization and propagation direction. At the input of this crystal, an electric field A_{opt} with optical frequencies is sent with a 45° polarization orientation relative to the axes X and Y, collinearly with a THz electric field A_{THz} polarized along X. Then, using the fact that both dephasings φ_x and φ_y are small, we connect with the notation of Sections 2 and 3 by the relationships

$$\begin{aligned} a_0(\omega) &= A_{2x}(\omega)\exp[ik(\omega)l] \\ &= A_{2y}(\omega)\exp[ik(\omega)l] \\ &\equiv A_{\mathrm{opt}}(\omega)\exp[ik(\omega)l], \end{aligned} \tag{51}$$

$$A_1(\Omega) \equiv A_{\mathrm{THz}}(\Omega). \tag{52}$$

For the case considered here and from Eqs. (40) and (41) we obtain

$$\begin{aligned} \varphi &= \varphi_y - \varphi_x \\ &= \int_{-\infty}^{+\infty} \frac{2\pi\omega^2}{c^2|k'(\omega)|} \chi^{(2)}_{\mathrm{eff}}(\omega; \Omega, \omega - \Omega) \\ &\quad \times \left\{ \frac{\exp[i\Delta k_+(\Omega, \omega)l] - 1}{i\Delta k_+(\Omega, \omega)} \right\} \\ &\quad \times \frac{A_{\mathrm{THz}}(\Omega)A_{\mathrm{opt}}(\omega - \Omega - \omega_0)}{A_{\mathrm{opt}}(\omega - \omega_0)} \exp(-i\Omega\tau)\mathrm{d}\Omega, \end{aligned} \tag{53}$$

with

$$\chi^{(2)}_{\mathrm{eff}} = \chi^{y}_{\mathrm{eff}} - \chi^{x}_{\mathrm{eff}}. \tag{54}$$

We require the absolute value $|k'(\omega)|$ in Eq. (53) to extend the integration of Eq. (50) from $-\infty$ to $+\infty$. We then obtain the EO signal by using Eq. (50):

$$\begin{aligned} S(\tau) = \frac{\epsilon_0 c}{2} \mathrm{Re} \int_{-\infty}^{+\infty} \int_{-\infty}^{+\infty} \frac{2\pi\omega^2}{c^2|k'(\omega)|} \exp[-2\beta(\omega)l] \\ \times \chi^{(2)}_{\mathrm{eff}}(\omega; \Omega, \omega - \Omega) \left\{ \frac{\exp[i\Delta k_+(\Omega, \omega)l] - 1}{i\Delta k_+(\Omega, \omega)} \right\} \\ \times A_{\mathrm{THz}}(\Omega)A^*_{\mathrm{opt}}(\omega - \omega_0)A_{\mathrm{opt}}(\omega - \Omega - \omega_0) \\ \times \exp(-i\Omega\tau)\mathrm{d}\Omega\mathrm{d}\omega, \end{aligned} \tag{55}$$

where the prefactor of 1/2 comes from changing the limits on the integral in Eq. (55) compared with those in Eq. (50). Equation (55) is rewritten more simply as

$$S(\tau) = \frac{\pi\epsilon_0}{c} \mathrm{Re} \int_{-\infty}^{+\infty} A_{\mathrm{THz}}(\Omega) f(\Omega) \exp(-i\Omega\tau)\mathrm{d}\Omega, \tag{56}$$

with

$$\begin{aligned} f(\Omega) = \int_{-\infty}^{+\infty} \frac{\omega^2}{|k'(\omega)|} \exp[-2\beta(\omega)l] \chi^{(2)}_{\mathrm{eff}}(\omega; \Omega, \omega - \Omega) \\ \times \left\{ \frac{\exp[i\Delta k_+(\omega, \Omega)l] - 1}{i\Delta k_+(\omega, \Omega)} \right\} \\ \times A^*_{\mathrm{opt}}(\omega - \omega_0)A_{\mathrm{opt}}(\omega - \Omega - \omega_0)\mathrm{d}\omega. \end{aligned} \tag{57}$$

Because $f(\Omega)$ is Hermitian, i.e., $f(-\Omega) = f^*(\Omega)$, the integral of Eq. (56) is real and the designation Re can be dropped. The final result for the EO signal then becomes

$$S(\tau) = \frac{\pi\epsilon_0}{c} \int_{-\infty}^{+\infty} A_{\mathrm{THz}}(\Omega) f(\Omega) \exp(-i\Omega\tau)\mathrm{d}\Omega. \tag{58}$$

The function $f(\Omega)$ expresses in the frequency domain the various experimental features of EO detection of THz pulses that can cause pulse distortion, loss of bandwidth, or both. If $f(\Omega)$ were frequency independent, the mea-

sured EO signal pulse $S(\tau)$ would be a replica of the THz pulse that is entering the EO crystal.[11] However, as can be seen from an inspection of the individual terms in Eq. (57), the measurement can be compromised by several factors. The spectral amplitudes can be changed and the measured pulse distorted by the frequency-dependent nonlinearity $\chi^{(2)}_{\text{eff}}$, by the strong THz absorption of the EO crystal, by the frequency-dependent coherence length, and by the spectral attenuation that is due to a too-broad (in the time domain) optical probing pulse. The distortions from $\chi^{(2)}_{\text{eff}}$ and THz absorption are especially strong if the THz spectrum overlaps the resonant frequencies of the EO crystal (see Appendix B).

5. APPROXIMATE SOLUTION

Consistent with the slowly varying envelope approximation used in this theoretical approach[8] and for the usual experimental situation in which the optical bandwidth of the interrogating light pulse is small compared with the optical carrier frequency, we can make an important simplification of our general result for the detected EO signal. In this case $\omega \approx \omega_0$; then, to a good approximation (see Appendix A), the more general expression of Eq. (58) for the EO signal simplifies to

$$S(\tau) = \frac{\pi\epsilon_0}{c}\frac{\omega_0^2}{k'(\omega_0)}\exp[-2\beta(\omega_0)l] \times \int_{-\infty}^{+\infty}\chi^{(2)}_{\text{eff}}(\omega_0;\Omega,\omega_0-\Omega) \times \left\{\frac{\exp[i\Delta k_+(\omega_0,\Omega)l]-1}{i\Delta k_+(\omega_0,\Omega)}\right\} \times A_{\text{THz}}(\Omega)C_{\text{opt}}(\Omega)\exp(-i\Omega\tau)\mathrm{d}\Omega, \quad (59)$$

where $C_{\text{opt}}(\Omega)$ is the autocorrelation of the optical electric field as shown below:

$$C_{\text{opt}}(\Omega) = \int_{-\infty}^{+\infty}A^*_{\text{opt}}(\omega-\omega_0)A_{\text{opt}}(\omega-\omega_0-\Omega)\mathrm{d}\omega. \quad (60)$$

The EO signal is then rewritten to be

$$S(\tau) \propto \int_{-\infty}^{+\infty}A_{\text{THz}}(\Omega)f(\Omega)\exp(-i\Omega\tau)\mathrm{d}\Omega, \quad (61)$$

where

$$f(\Omega) = C_{\text{opt}}(\Omega)\chi^{(2)}_{\text{eff}}(\omega_0;\Omega,\omega_0-\Omega) \times\left\{\frac{\exp[i\Delta k_+(\omega_0,\Omega)l]-1}{i\Delta k_+(\omega_0,\Omega)}\right\}. \quad (62)$$

This result expresses the time-dependent EO signal $S(\tau)$ as a relatively simple Fourier integral, which is easily evaluated. However, as we shall see in Section 7 below, for many applications the actual time-dependent pulse $S(\tau)$ is of less interest than the corresponding complex spectrum $S(\Omega)$.

Here, again, $f(\Omega)$ shows the effect on the EO signal of the various parameters of the EO technique. If $f(\Omega)$ were independent of frequency, $S(\tau)$ would be a faithful replica of the incoming THz pulse that is entering the EO crystal.[11] Here, for the approximate solution for which $\Delta\omega \ll \omega_0$, $f(\Omega)$ is the product of three frequency-dependent terms that act as spectral filters on the incoming THz complex spectral amplitude $A_{\text{THz}}(\Omega)$. The first $C_{\text{opt}}(\Omega)$ is the complex spectrum of the autocorrelation of the probing light pulse. For the usual case the optical bandwidth $\Delta\omega$ is much larger than the THz bandwidth, so this term has little effect. The frequency-dependent $\chi^{(2)}_{\text{eff}}$ can distort the incoming THz spectrum, as shown in Appendix B. The term enclosed by braces in Eq. (62) reduces to the well-known parametric result,[8] $l\,\text{sinc}(\Delta k_+ l/2)$, for real Δk_+, whereas the imaginary part of Δk_+ describes the usually strong absorption of the THz radiation by the EO crystal. The effect of this term is reduced by the EO crystal thickness l being made as small as possible. In the limit of small thickness, relation (61), including the frequency-dependent $\chi^{(2)}_{\text{eff}}$, is similar to the result obtained by Auston and Nuss.[12] The combined effect of all these terms can distort the EO signal and reduce and cause discontinuities in the corresponding measured THz spectrum. These factors must all be considered in relating the measured EO signal to the incoming THz pulse.

6. COMPARISON WITH PREVIOUS RESULTS

By rewriting our frequency-domain evaluation of the EO signal $S(\tau)$ as given in relation (61) in the time domain, we obtain a more general description of the intuitive time-domain picture that was introduced by Bakker *et al.*[9] For this we need now to introduce the concept of group velocity v_g of the optical probing pulse.[8,9,13] If the dispersion is small for the wave vector of the optical pulse, we can use the approximations

$$k(\omega_0+\Delta\omega) \approx k(\omega_0) + \left(\frac{\mathrm{d}k}{\mathrm{d}\omega}\right)_{\omega_0}\Delta\omega,$$

$$\frac{\mathrm{d}k}{\mathrm{d}\omega} = \frac{1}{v_g} \equiv \frac{n_g}{c}. \quad (63)$$

Then, following Nahata *et al.*[13] or Wu and Zhang,[14] we can rewrite Eq. (20) in the simpler approximate form as

$$\Delta k_+ = -k(\omega_0+\Omega)+k(\Omega)+k(\omega_0) \approx -k(\omega_0)-\Omega\left(\frac{\mathrm{d}k}{\mathrm{d}\omega}\right)_{\omega_0}+k(\Omega)+k(\omega_0) \approx k(\Omega)-k_g(\Omega), \quad (64)$$

where we define the wave vector $k_g(\Omega)$ of the envelope of the optical field to be

$$k_g(\Omega) \equiv \Omega\left(\frac{\mathrm{d}k}{\mathrm{d}\omega}\right)_{\omega_0} = \frac{\Omega}{v_g} = \frac{\Omega}{c}n_g. \quad (65)$$

Relation (61) can now be shown to be equivalent to

$$S(\tau) \propto \int_0^l dz \int_{-\infty}^{+\infty} C_{opt}(\Omega) \times \exp[-ik_g(\Omega)z]\chi^{(2)}_{eff}(\omega_0; \Omega, \omega_0 - \Omega)A_{THz}(\Omega) \times \exp[ik(\Omega)z]\exp(-i\Omega\tau)d\Omega; \quad (66)$$

i.e., the integration with respect to z of relation (66) gives relation (61). Relation (66) is then equivalent to the following correlation:

$$S(\tau) \propto \int_0^l dz \int_{-\infty}^{+\infty} I_{opt}(z, t - \tau)P_{EO}(z, t)dt, \quad (67)$$

where

$$P_{EO}(z, t) \propto \int_{-\infty}^{+\infty} \chi^{(2)}_{eff}(\omega_0; \Omega, \omega_0 - \Omega)A_{THz}(\Omega) \times \exp[ik(\Omega)z]\exp(-i\Omega t)d\Omega. \quad (68)$$

$P_{EO}(z, t)$ is designated as the propagating EO pulse, which linearly propagates through the crystal, similarly to the THz pulse. However, as we can see from relation (68), the pulse shape of the EO pulse can be quite different from that of the THz pulse, especially if the frequency components of the THz pulse overlap resonance frequencies of the EO susceptibility $\chi^{(2)}_{eff}$, as shown in Appendix B. It is informative to note that $C_{opt}(\Omega)$, which is an autocorrelation in the frequency domain, appears as the product of optical fields I_{opt}, which is proportional to the intensity of the optical pulse in the time domain, as shown in relation (67). Therefore I_{opt} is given by

$$I_{opt}(t) = |A_{opt}(t)|^2, \quad (69)$$

$$I_{opt}(z, t) = \exp(-2\beta_0 z)I_{opt}(z = 0, t - z/v_g). \quad (70)$$

Equation (70) indicates that $I_{opt}(t)$ propagates with group velocity v_g and is attenuated by optical absorption β_0 of the EO crystal.

The result for EO signal $S(\tau)$ as expressed in relation (67) has the intuitively appealing interpretation of the cross correlation between the interrogating optical pulse traveling at the optical group velocity and the propagating EO pulse (see Fig. 3) integrated over the EO crystal length. It is clear from Fig. 3 that measuring the EO pulse requires that the time duration of $I_{opt}(t)$ be significantly less than the temporal features of the EO pulse.

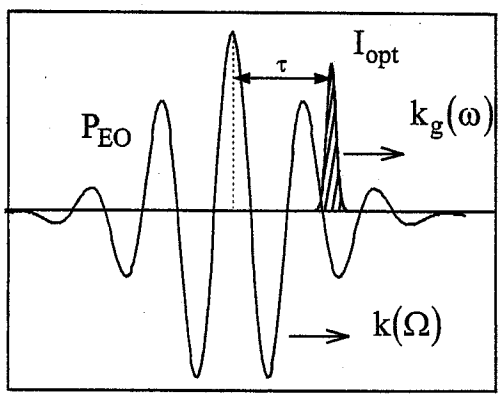

Fig. 3. Propagation of optical intensity I_{opt} and EO pulse P_{EO} in the nonlinear crystal.

This requirement shows that the bandwidth $\Delta\omega$ of the optical pulse should be much larger than the bandwidth of the THz pulse. For the usual experimental situation one can easily satisfy this requirement while keeping $\Delta\omega$ much less than the carrier frequency ω_0. This time-domain picture was introduced by Bakker *et al.*,[9] and our result of relation (67) reduces identically to their result for their case of a frequency-independent $\chi^{(2)}_{eff}$, for which the EO pulse has the same shape as the THz pulse.

7. TERAHERTZ TIME-DOMAIN SPECTROSCOPY WITH ELECTRO-OPTIC DETECTION

Because of the possibly strong time-domain distortion of the measured EO signal compared with the THz pulse incident upon the EO crystal, the general applicability of the THz TDS technique[1] was previously unclear. Using the complete frequency-domain evaluation of the EO signal of Eq. (58), we now show that it is possible to perform THz TDS with EO detection.

For THz TDS, two EO signals are measured, with and without the investigated sample in place. Let $H(\Omega)$ be the desired complex spectral transmission function of the sample in the THz range. If the complex amplitude spectrum of the THz field at the input to the sample is $A_{In}(\Omega)$, then the spectrum at the output is $A_{Out}(\Omega) = H(\Omega)A_{In}(\Omega)$. Given that the detected EO signal is described by Eq. (58), we obtain $S_{sample}(\tau)$ and $S_{ref}(\tau)$ with and without the sample, respectively. Then the complex amplitude spectra of S_{sample} and S_{ref} yield[11]

$$S_{ref}(\Omega) = \frac{\pi\epsilon_0}{c} t_{12}(\Omega)A_{In}(\Omega)f(\Omega), \quad (71)$$

where $t_{12}(\Omega)$ is the complex Fresnel transmission coefficient for the THz pulse into the EO crystal, and

$$S_{sample}(\Omega) = \frac{\pi\epsilon_0}{c} H(\Omega)t_{12}(\Omega)A_{In}(\Omega)f(\Omega). \quad (72)$$

The following ratio eliminates the transmission coefficient $t_{12}(\Omega)$ and the filter function $f(\Omega)$ that describes the EO detection and gives the spectral transmission of the sample:

$$\frac{S_{sample}(\Omega)}{S_{ref}(\Omega)} = H(\Omega). \quad (73)$$

From Eq. (73) we clearly see that the ratio of the complex spectral amplitudes gives the desired $H(\Omega)$ function that describes the sample. Even though $f(\Omega)$ has been mathematically eliminated because of the EO detection, the spectral coverage may not be continuous, mainly as the result of the absorption of THz radiation by the EO crystal and to a lesser extent because of phase mismatch and of the frequency dependence of the EO susceptibility, as shown in Appendix B.

Practically speaking, the applications of EO detection to THz TDS will depend on the signal-to-noise ratio of the complex amplitude spectrum of the measured reference pulse, independently of the fact that the EO signal may not be a replica of the THz pulse that is entering the EO

crystal. Although the EO signal and the corresponding complex spectra are determined by the incoming THz pulse, the signal is also determined by the type, orientation, and thickness of the EO crystal and by the pulse width and the carrier frequency of the interrogating optical pulse. The corresponding spectrum may then have regions of low signal or gaps in the coverage.

8. CONCLUSION

We have presented a complete frequency-domain description of electro-optic detection of terahertz electromagnetic radiation, including a description of the ellipsometry technique employed. These frequency-domain results show the effect of EO detection of a pulse of THz radiation as the product of three spectral filters acting on the complex amplitude spectrum of the THz pulse that is entering the EO crystal. If the product of these filter functions had a smooth spectral response much broader than the incoming spectrum of the THz pulse, the measured EO signal would be essentially the same as the THz pulse that was entering the EO crystal.[11] However, usually such is not the case. The first filter function describes the spectrum of the autocorrelation of the optical probing pulse, which is usually much broader than the spectrum of the measured THz pulse. Consequently, this filter has little detrimental effect on the EO measurement. The second filter describes the frequency dependence of the EO susceptibility $\chi^{(2)}_{\text{eff}}$, which can be strongly frequency dependent, as shown in Appendix B, and can thereby distort the EO signal and the corresponding spectrum, independently of the thickness of the EO crystal. The third filter describes the frequency-dependent coherence length determined by the mismatch between the optical probing pulse that is traveling at the optical group velocity and the frequency components of the propagating THz pulse. This filter function produces the usual Maker fringes and includes the absorption of the propagating THz radiation in the EO crystal. The effect of this filter can be reduced by a decrease in the thickness of the EO crystal. The combined effect of these three filters must be considered when the measured EO signal is related to the incoming THz pulse.[11] Independently of whether there is a substantial time-domain distortion of the measured EO signal compared with the THz pulse, this analysis shows that the usual procedures of THz TDS are applicable. The THz TDS analysis involves only the ratios of the complex amplitude spectra of the measured EO signals.

For the usual experimental situation in which the optical bandwidth of the interrogating light pulse is small compared with the optical carrier frequency, we have obtained an important simplification of our general frequency-domain result for the detected EO signal. When the Fourier integral that describes this simplified result is rewritten in the time domain, we obtain a more general description of the intuitive time-domain picture that was introduced by Bakker *et al.*[9] Restricting our time-domain result to the earlier frequency-independent EO susceptibility situation,[9] we identically obtain their intuitive picture, in which the EO signal is given by a cross correlation between the interrogating optical intensity pulse traveling at the optical group velocity and the propagating THz pulse integrated over the EO crystal length.

APPENDIX A: INFLUENCE OF THE SPECTRAL WIDTH OF THE OPTICAL PROBE PULSE

Let us consider no dispersion, constant absorption, and a perfect velocity match. Then $f(\Omega)$ described in Eq. (57) becomes proportional to

$$f(\Omega) \propto \int_{-\infty}^{+\infty} \omega A^*_{\text{opt}}(\omega - \omega_0) A_{\text{opt}}(\omega - \omega_0 - \Omega) \mathrm{d}\omega. \quad \text{(A1)}$$

Our goal in this appendix is to describe the accuracy of the approximation that we used to obtain Eq. (59) and more precisely the influence of the multiplication by ω in relation (A1). Let A_{opt} be a Gaussian pulse:

$$A_{\text{opt}}(\omega) = \frac{1}{\sqrt{\pi \Delta\omega^2}} \exp\left(-\frac{\omega^2}{\Delta\omega^2}\right). \quad \text{(A2)}$$

Relation (A1) yields

$$\begin{aligned} f(\Omega) &\propto \frac{1}{\pi\Delta\omega^2} \int_{-\infty}^{+\infty} \omega \\ &\quad \times \exp\left\{-\frac{1}{\Delta\omega^2}[(\omega - \omega_0)^2 + (\omega - \omega_0 - \Omega)^2]\right\} \mathrm{d}\omega \\ &\propto \frac{1}{\pi\Delta\omega^2} \int_{-\infty}^{+\infty} \omega g(\omega) \mathrm{d}\omega, \end{aligned} \quad \text{(A3)}$$

with

$$\begin{aligned} g(\omega) = \exp\Big\{ &-\frac{1}{\Delta\omega^2}[2\omega^2 - 2\omega(2\omega_0 + \Omega) + \omega_0^2 \\ &+ (\omega_0 + \Omega)^2]\Big\}. \end{aligned} \quad \text{(A4)}$$

Noticing that

$$\frac{\mathrm{d}g}{\mathrm{d}\omega} = -\frac{1}{\Delta\omega^2}(4\omega - 4\omega_0 - 2\Omega) g(\omega), \quad \text{(A5)}$$

we obtain

$$\int_{-\infty}^{+\infty} \omega g(\omega) \mathrm{d}\omega = \left(\omega_0 + \frac{\Omega}{2}\right) \int_{-\infty}^{+\infty} g(\omega) \mathrm{d}\omega. \quad \text{(A6)}$$

Then

$$f(\Omega) \propto \frac{1}{\Delta\omega\sqrt{2\pi}} \left(\omega_0 + \frac{\Omega}{2}\right) \exp\left(-\frac{\Omega^2}{2\Delta\omega^2}\right). \quad \text{(A7)}$$

Then, to a very good approximation ($\Omega \ll \omega_0$),

$$f(\Omega) \propto \frac{1}{\Delta\omega\sqrt{2\pi}} \omega_0 \exp\left(-\frac{\Omega^2}{2\Delta\omega^2}\right) = \omega_0 C_{\text{opt}}(\Omega). \quad \text{(A8)}$$

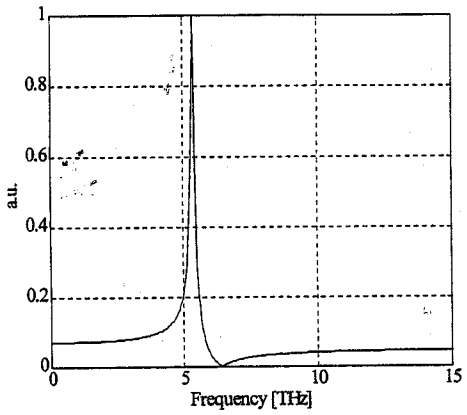

Fig. 4. Absolute value of the second-order susceptibility in ZnTe.

APPENDIX B: FREQUENCY DEPENDENCE OF $\chi^{(2)}_{\text{eff}}$

The frequency dependence of the effective nonlinear susceptibility $\chi^{(2)}_{\text{eff}}$ can be approximated in the THz domain by an extension[15] of the well known Miller rule. Using

$$\chi \equiv \chi^e + \chi^i = \frac{\epsilon}{\epsilon_0} - 1, \quad \chi^e \equiv n^2 - 1,$$

and

$$\chi^i = \frac{\epsilon}{\epsilon_0} - n^2, \tag{B1}$$

we obtain

$$\chi^{(2)}_{ijk}(\Omega) = \chi^e_i(\omega_0)\chi^e_j(\omega_0)[\delta^e_{ijk}\chi^e_k(\Omega) + \delta^i_{ijk}\chi^i_k(\Omega)]. \tag{B2}$$

The coefficients δ^e_{ijk} and δ^i_{ijk} are frequency independent and depend on the nonlinear crystal. The effective nonlinear susceptibility $\chi^{(2)}_{\text{eff}}$ can be estimated from Eq. (B2) and the linear susceptibilities in the optical domain [$\chi^e_i(\omega_0)$ and $\chi^e_j(\omega_0)$] and in the THz domain [$\chi^e_k(\Omega)$ and $\chi^i_k(\Omega)$].

As a specific example, we can use Eq. (B2) for ZnTe crystals. The normalized second-order susceptibility in ZnTe, for which the linear susceptibility of ZnTe (Ref. 16) is used and δ^e_{ijk} is assumed to equal δ^i_{ijk}, is shown in Fig. 4.

Clearly, the frequency dependence shown in Fig. 4 can cause extreme distortion of the measured EO signal pulse $S(\tau)$ compared with the incident THz pulse if the frequency spectrum of the incoming THz pulse overlaps the resonance at 5.3 THz. Also, note the amplitude drop on the high-frequency side of the resonance compared with that on the low-frequency side.

ACKNOWLEDGMENTS

We acknowledge careful readings of this manuscript and many helpful and stimulating suggestions by R. Alan Cheville, Roger W. McGowan, Rajind Mendis, and Jiang-Quan Zhang. This study was partially supported by the National Science Foundation under grants PHY-9422952 and PHY-9731201.

REFERENCES AND NOTES

1. D. Grischkowsky, S. Keiding, M. van Exter, and Ch. Fattinger, "Far-infrared time-domain spectroscopy with terahertz beams of dielectrics and semiconductors," J. Opt. Soc. Am. B **7**, 2006–2015 (1990).
2. D. M. Mittleman, R. H. Jacobsen, and M. C. Nuss, "T-ray imaging," IEEE J. Sel. Top. Quantum Electron. **2**, 679–692 (1996).
3. Q. Wu, T. D. Hewitt, and X.-C. Zhang, "Two-dimensional electro-optic imaging of THz beams," Appl. Phys. Lett. **69**, 1026–1028 (1996).
4. R. A. Cheville, R. W. McGowan, and D. Grischkowsky, "Late-time target response measured with terahertz impulse ranging," IEEE Trans. Antennas Propag. **45**, 1518–1524 (1997).
5. Q. Wu and X.-C. Zhang, "Free-space electro-optics sampling of mid-infrared pulses," Appl. Phys. Lett. **71**, 1285–1286 (1997).
6. Y. Cai, I. Brener, J. Lopata, J. Wynn, L. Pfeiffer, J. B. Stark, Q. Wu, X. C. Xhang, and J. F. Federici, "Coherent terahertz radiation detection: direct comparison between free-space electro-optic sampling and antenna detection," Appl. Phys. Lett. **73**, 444–446 (1998).
7. S.-G. Park, M. R. Melloch, and A. M. Weiner, "Comparison of terahertz waveforms measured by electro-optic and photoconductive sampling," Appl. Phys. Lett. **73**, 3184–3186 (1998).
8. Y. R. Shen, *The Principles of Nonlinear Optics* (Wiley, New York, 1984).
9. H. J. Bakker, G. C. Cho, H. Kurz, Q. Wu, and X.-C. Zhang, "Distortion of terahertz pulses in electro-optic sampling," J. Opt. Soc. Am. B **15**, 1795–1801 (1998).
10. M. Born and E. Wolf, *Principles of Optics* (Pergamon, London, 1987).
11. Clearly the frequency spectrum $A_{\text{THz}}(\Omega)$ of the THz pulse that is entering the EO crystal is equal to the incident spectrum $A_{\text{In}}(\Omega)$ multiplied by the complex frequency-dependent Fresnel transmission coefficient $t_{12}(\Omega)$ that describes the EO crystal; i.e., $A_{\text{THz}}(\Omega) = t_{12}(\Omega)A_{\text{In}}(\Omega)$. See Section 7.
12. D. H. Auston and M. C. Nuss, "Electrooptic generation and detection of femtosecond electrical transients," IEEE J. Quantum Electron. **24**, 184–197 (1988).
13. A. Nahata, A. S. Weling, and T. F. Heinz, "A wideband coherent terahertz spectroscopy system using optical rectification and electro-optic sampling," Appl. Phys. Lett. **69**, 2321–2323 (1996).
14. Q. Wu and X.-C. Zhang, "7 terahertz broadband GaP electro-optic sensor," Appl. Phys. Lett. **70**, 1784–1786 (1997).
15. G. D. Boyd and M. A. Pollack, "Microwave nonlinearities in anisotropic dielectrics and their relation to optical and electro-optical nonlinearities," Phys. Rev. B **7**, 5345–5359 (1973).
16. T. Hattori, Y. Homma, A. Mitsushi, and M. Tacke, "Indices of refraction of ZnS, ZnSe, ZnTe, CdS, and CdTe in the far infrared," Opt. Commun. **7**, 229–232 (1973).